JOURNAL OF GEOPHYSICAL RESEARCH, VOL. 101, NO. E7, PAGES 16,881–16,889, JULY 25, 1996

Transport timescales in the Martian atmosphere: General circulation model simulations

Jeffrey R. Barnes and Thomas D. Walsh

College of Oceanic and Atmospheric Sciences, Oregon State University, Corvallis

James R. Murphy[1]

San Jose State University Foundation, San Jose, California

Abstract. Simulations with a Mars general circulation model (GCM) are used to perform idealized tracer transport experiments, which are analyzed to yield estimates of eddy mixing coefficients as well as "stratospheric" ventilation timescales for the zonal-mean circulation. The results indicate that relatively moderate values of the vertical eddy mixing coefficient, $K_z \sim$ 20–100 m^2/s, may be most appropriate for the 10 to 45-km altitude region of the Martian atmosphere. Under dusty solstice conditions, somewhat stronger eddy mixing is present, but the transport is dominated by advection by the mean meridional circulation which acts to ventilate the atmosphere above 1 mbar (~20 km) in only about 7 days. Such a mean circulation has transport effects which are roughly comparable to those produced by eddy mixing with a much larger K_z value, ~1500 m^2/s. In contrast, the computed mean ventilation timescale for a nondusty equinox circulation is approximately 180 days. In this case, vertical eddy mixing is the dominant transport process. In an intermediate nondusty solstice case, the effects of mean advection and eddy mixing are of comparable importance. An estimate of a mean ventilation timescale from the GCM for a late northern winter seasonal date (~45 days) is in very good agreement with the value of ~38 days recently inferred from Mariner 9 infrared imaging spectrometer (IRIS) data [*Santee and Crisp*, 1995].

1. Introduction

The transport of trace constituents by the atmospheric circulation on Mars is of key importance for many problems related to the composition and structure of the atmosphere and the current and past climates of the planet. Dust and water transports are central to an understanding of the climate system [e.g., *Kahn et al.*, 1992; *Jakosky and Haberle*, 1992], while the processes that act to maintain the dominantly CO_2 atmosphere crucially involve atmospheric transport and mixing [e.g., *Kong and McElroy*, 1977].

At present, the observational data that allow insight into atmospheric transport processes on Mars are quite limited. There are no direct wind observations, except at the two Viking Lander sites. Observations of the atmospheric thermal structure, as by the Mariner 9 infrared imaging spectrometer (IRIS), allow the zonal winds to be estimated and can also permit mean winds in the meridional plane of the atmosphere to be inferred [*Santee and Crisp*, 1995]. A number of previous studies have made inferences about the strength of atmospheric mixing and transport processes, by examining dust and ice hazes [*Conrath*, 1975; *Toon et al.*, 1977; *Anderson and Leovy*, 1978; *Kahn*, 1990; *Chassefiere et al.*, 1992; *Korablev et al.*, 1993].

The objective of the present study is to make use of numerical simulations of the Martian atmospheric circulation with a general circulation model (GCM) and tracer transport experiments with an aerosol model to examine some of the basic aspects of the transport processes. The complete nature of the model results allows the estimation of eddy mixing coefficients, as well as the characterization of the advective transport by the zonal-mean circulation.

2. Approach

The basic approach employed is to perform numerical simulations of the atmospheric circulation with a GCM, and use these to conduct simulations of tracer transport with an aerosol model. The results from the latter are analyzed to yield the desired transport mea-

[1]Also at NASA Ames Research Center, Moffett Field, California.

Paper number 96JE00500.
0148-0227/96/96JE-00500$09.00

sures. The zonally averaged transport equation for a tracer q can be expressed in the following form, in log pressure coordinates,

$$\frac{\partial \overline{q}}{\partial t} + \overline{v}\frac{\partial \overline{q}}{\partial y} + \overline{w}\frac{\partial \overline{q}}{\partial z} = -\frac{1}{p}\nabla \cdot \mathbf{F}$$

where $\mathbf{F}$ is the eddy flux vector,

$$\mathbf{F} = (\overline{pv'q'}, \overline{pw'q'})$$

The flux-gradient relation then connects the known (from the GCM and transport model data) eddy fluxes with the to-be-determined eddy mixing tensor $\tilde{K}$,

$$(F_y, F_z) = -p\tilde{K} \cdot \nabla \overline{q}$$

Plumb [1979] and *Matsuno* [1980] have shown that the flux-gradient relationship is valid for small-amplitude eddies on a zonal flow. For the Earth's atmosphere, the study of *Plumb and Mahlman* [1987] lends considerable support to the utility of the above relation for generalized eddy motions, as does the study of *Shia et al.* [1989]. Of course, for nonconservative tracers the eddy mixing tensor will generally be tracer-dependent [see *Plumb and Mahlman*, 1987].

The GCM utilized is the current version of the NASA Ames Mars GCM, a state-of-the-art model of the atmospheric circulation and climate. *Pollack et al.* [1990] present a summary of the technical details of this model, which incorporates "static" atmospheric dust loadings. The current version of the Mars GCM has 13 vertical levels extending to a height of ~45–50 km, and a horizontal grid spacing of 7.5° latitude by 9° longitude. The static atmospheric dust (the mixing ratio of which depends only on pressure in the experiments here) strongly influences both the solar and IR radiative heating/cooling of the atmosphere, and thus the thermal structure and circulation simulated by the GCM [e.g., *Pollack et al.*, 1990; *Haberle et al.*, 1993]. Both dusty and nondusty GCM simulations have been analyzed in the present study.

The tracer transport simulations have been performed using the aerosol transport model of *Toon et al.* [1988]. *Murphy et al.* [1995] present a brief summary of this model, as it is adapted for use with the Mars GCM. The model provides a host of capabilities in the realm of microphysical and chemical processes, but for this study none of these are invoked. In particular, there is no sedimentation of the tracer and no removal of tracer mass at the ground (the fluxes at the surface vanish), and no subgrid convective mixing is allowed to take place in the transport model. No explicit diffusion is incorporated in the version of the aerosol model used for this study. The version used thus simulates the conservative and passive transport of a tracer field (e.g., a completely inert chemical species) by the resolved winds in the GCM. The neglect of convective mixing means that the vertical transport may be substantially underestimated in much of the lowest 5–10 km of the atmosphere. The focus here is on the large-scale transport at higher levels (10–40 km) in the Martian atmosphere.

The aerosol model was run in parallel with the Mars GCM, as described by *Murphy et al.* [1995], but in a strictly "one-way" mode (the tracer field having no influence on the GCM). In order to allow the estimation of the full eddy transport tensor, two transport experiments with very different initial conditions were performed for each circulation case (as in *Plumb and Mahlman* [1987]). One initial tracer state was purely vertically stratified, while the second varied only in latitude. The transport simulations were carried out for 10-day periods, corresponding to days 31–40 of the GCM runs. The GCM "spins up" extremely rapidly because of the very short radiative relaxation times in the Martian atmosphere, and days 21–50 have previously been utilized for extensive analyses of the circulation [e.g., *Haberle et al.*, 1993; *Barnes et al.*, 1993, 1996].

The short length of the transport simulations reflects the rapid nature of the transport processes; longer simulations would have required the use of a forcing/damping to prevent the tracer field from becoming overly well mixed (thus interfering with the determination of the eddy transport tensor, as discussed by *Plumb and Mahlman* [1987]). Longer simulations would have been desirable, certainly, for some of the eddy motions which could be characterized by relatively longer timescales [see *Barnes et al.*, 1993]. For such motions, the chosen 10-day period may not necessarily be very representative of the longer-term behavior. Various eddy statistics (e.g., zonally averaged heat and momentum fluxes), however, show remarkably low variability from one particular 10-day period to another, after the initial 20 days of spinup. There is no evidence that the Mars GCM exhibits variations that might make a 10-day interval unrepresentative for the mean circulation.

The data from the transport model were interpolated to constant pressure surfaces, and the analyses to determine the eddy transport tensor were then performed (essentially as by *Plumb and Mahlman* [1987]). The eddy fluxes and zonal-mean tracer gradients were averaged over the 10-day runs, leading to average values for the transport coefficients. Because of the very large topography in the Mars GCM, the interpolation to pressure levels presented difficulties. Many of the data for the lowest several model levels had to be extrapolated from higher levels, and this resulted in rather noisy and unreliable determinations of the transport coefficients when these values were included. All "subsurface" points were thus excluded from the analyses, and values of the transport coefficients were determined only above ~5 km. (The transport model itself is in sigma coordinates and the tracer transport is correctly represented (there are no fluxes through the boundaries) at lower levels, given the neglect of convective and other small-scale mixing.)

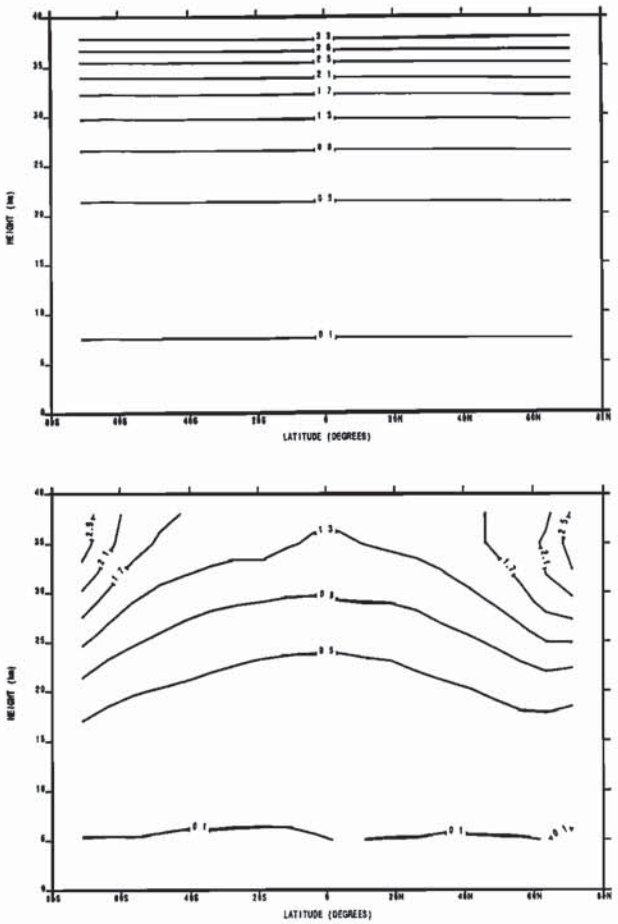

Figure 1. Zonally averaged tracer mixing ratios (top) for the initial state and (bottom) for day 10 of the equinox transport experiment with a vertically stratified tracer. The absolute values are arbitrary.

3. Results

Three GCM simulations were used for the present study: a near-equinox ($L_s \sim 358°$) run with no dust and no condensation flow, a northern winter solstice ($L_s \sim 274°$) run with no dust, and a northern winter solstice simulation with substantial dustiness (a dust opacity of one). The near-equinox simulation represents a weak circulation regime [see *Haberle et al.*, 1993], a "minimum transport" case, while the solstice runs exhibit substantially stronger circulations.

Figure 1 shows the initial and final zonal-mean tracer fields from the near-equinox experiment with a vertically stratified tracer. The basic evolution of the tracer distribution reflects the structure of the mean meridional circulation, with upward advection in lower latitudes and downward transport at higher latitudes in both hemispheres. In this case the mean meridional circulation, as shown in Figure 2, is beginning to approach a double Hadley cell configuration which is relatively symmetric about the equator, similar to that in the two near-equinox experiments examined by *Haberle et al.* [1993]. The northern Hadley cell is significantly stronger at lower levels (below ~10 km) and extends well into the southern hemisphere in the simulation here, but at higher levels (above ~15 km) the two cells are quite symmetric with maximum rising motion occurring near the equator. The vertical motions are of the order of 0.5 cm/s, while the mean meridional flow is ~1–2 m/s. The time and zonally averaged eddy tracer fluxes (not shown) in the near-equinox experiment with a vertically stratified tracer are strongly downgradient and are largest in low latitudes. The strong vertical eddy mixing in this region acts to keep the vertical gradients from becoming steeper at upper levels, in the presence of the mean advective fluxes.

Figure 3 shows the initial and day 6 zonal-mean tracer fields from the dusty northern winter solstice experiment with a meridionally stratified tracer. Again, the basic evolution of the tracer field reflects the structure of the mean circulation in the models, with a very strong overturning of the tracer contours in low and middle latitudes being evident. In this case the mean circulation is dominated by an intense cross-equatorial Hadley cell extending throughout the entire depth of the model, as

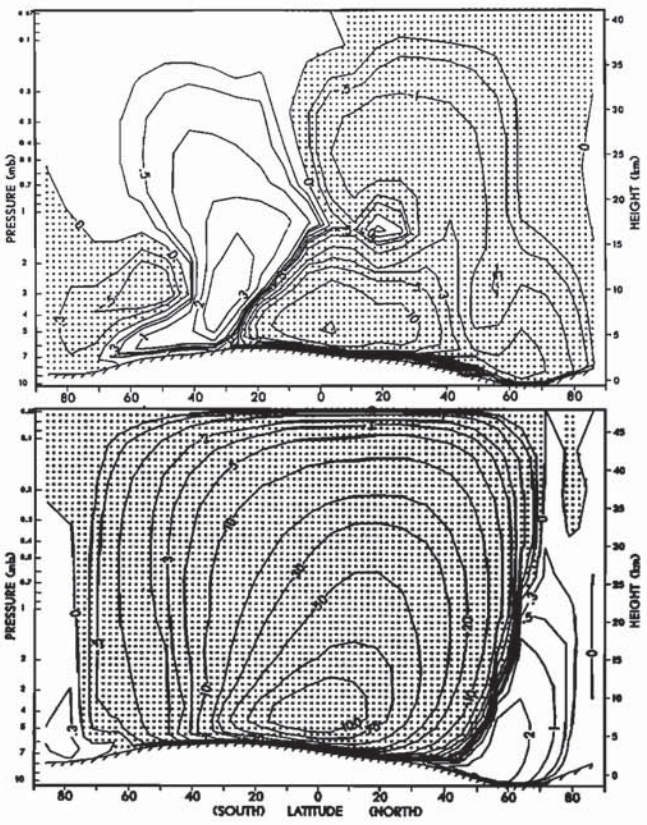

Figure 2. Mass stream functions for the (Eulerian) mean meridional circulation in the (top) nondusty near-equinox and (bottom) dusty solstice simulations. The units of the values are 10^8 kg/s, and shaded regions correspond to circulations in a clockwise sense. The contour intervals are not uniform.

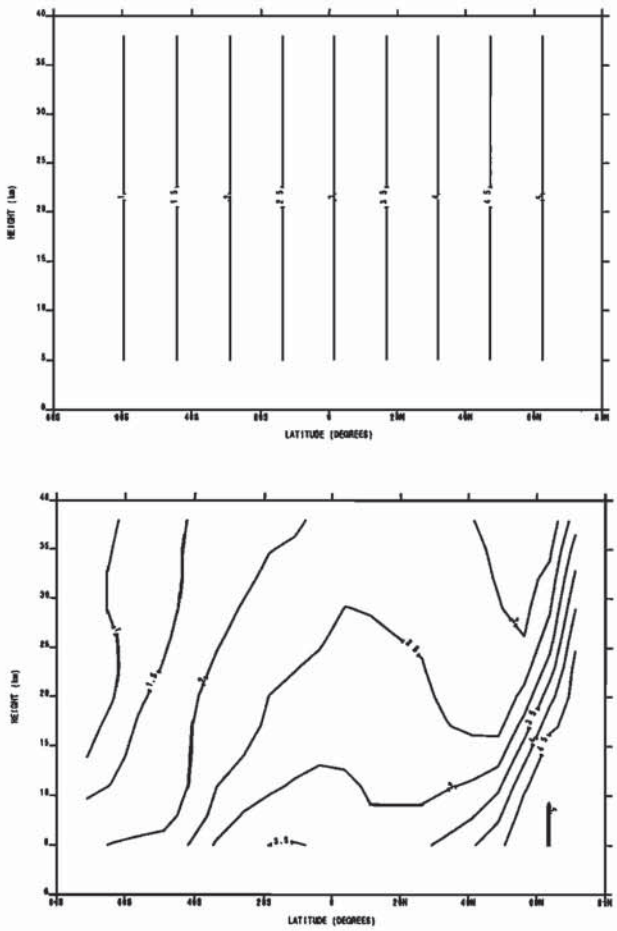

Figure 3. Zonally averaged tracer mixing ratios (top) for the initial state and (bottom) for day 6 of the dusty solstice transport experiment with a latitudinally stratified tracer.

shown in Figure 2. The mean vertical motions in this cell are in the range of ~2–12 cm/s, peaking at high levels, while the mean meridional flows are of the order of 5–20 m/s, with peak wind speeds in excess of 50 m/s near the model top in the northern subtropics. By day 6, the tracer contours in the experiment with a vertically stratified field (not shown) are beginning to become roughly parallel in many regions to those in Figure 3, reflecting the extremely short timescales on which the fields are being "wrapped up" by the Hadley circulation. Under these conditions, the determination of the eddy mixing tensor begins to become difficult.

The evolution of the zonal-mean tracer fields in the nondusty solstice experiments (not shown) is qualitatively similar to that in the dusty solstice experiments, but is much less rapid. In this intermediate transport case, the mean meridional winds are ~1–5 m/s, with vertical motions in the range of ~0.5–2.5 cm/s. The Hadley cell circulation is much less deep than it is in the dusty solstice case, with the strongest mean meridional flows located below 20-km altitude.

Tables 1 and 2 summarize some of the basic results from the analyses of the transport experiments. The transport by the mean meridional circulation has been characterized by a "ventilation" or overturning timescale for the model "stratosphere" (the region above 1 mbar, or ~18 km), estimated as by *Santee and Crisp* [1995]. That is, the upward mass flux into this region has been calculated separately for each experiment and used to obtain the ventilation timescale value (the stratospheric mass divided by the mass flux). Characteristic values for the vertical and meridional eddy mixing coefficients are given along with corresponding timescales in Table 1, the latter calculated for a vertical length scale equal to the pressure scale height and a meridional length scale equal to the planetary radius ($\tau_z = H^2/K_{zz}$ and $\tau_y = a^2/K_{yy}$). Also given in Table 2 is the ventilation timescale computed for an additional GCM experiment, one for a late northern winter seasonal date ($L_s \sim 345°$) with a dust optical depth of 0.3. This case allows a direct comparison with the results obtained by *Santee and Crisp* [1995] from Mariner 9 IRIS data.

The values in Table 1 exhibit a very large variation with seasonal date and dust loading. The relatively sluggish mean circulation in the equinox case is characterized by a ventilation timescale of ~180 days, while for the nondusty solstice case this timescale is ~60 days. For the extremely intense circulation in the dusty case, the mean ventilation timescale is only about 1 week. Such a timescale is incredibly short by comparison with the Earth's stratosphere, where ventilation timescales are of the order of 1–2 years [*Shia et al.*, 1989]. The results in Table 1 indicate that tracer transport by mean advection and eddy mixing processes are of roughly comparable importance in the model atmosphere above ~10 km in the near-equinox and nondusty solstice cases, though vertical eddy mixing appears to be the more rapid process in the former simulation (especially at lower latitudes, as discussed below). In the

Table 1. Eddy Mixing Timescales

	Equinox	Solstice	Dusty Solstice
K_{zz}	~20–80 m^2/s	~30–120	~50–200
K_{yy}	~0.5–2.5 × 10^6 m^2/s	~1–3 × 10^6	~1–5 × 10^6
τ_z	~15–60 days	~10–40	~6–24
τ_y	~50–250 days	~40–120	~25–120

Table 2. Mean Ventilation Timescales

	Value, days
Equinox	~180
Solstice	~60
Dusty solstice	~7
Late northern winter	~45

dusty solstice experiment the mean advection is much faster than the eddy mixing, except in several limited regions, where the mixing is very intense (see below). The ventilation timescale for the late northern winter GCM case is about 45 days, which is in quite good agreement with the estimate of ~38 days obtained by *Santee and Crisp* [1995] using Mariner 9 IRIS data. A slightly higher dust opacity in this experiment would yield a slightly shorter timescale, though Sante and Crisp found a significantly nonuniform (in the horizontal) opacity.

There are large variations in latitude and height in the determined values of the eddy mixing coefficients

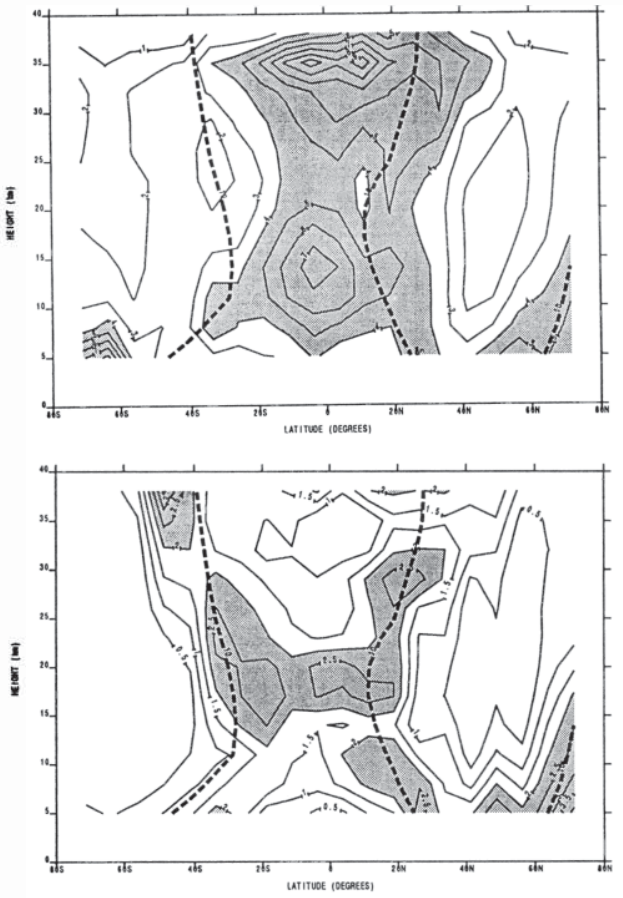

Figure 4. Latitude-height distribution of eddy mixing coefficients for the equinox case: (top) K_{zz} (in units of 10 m^2/s) and (bottom) K_{yy} (in units of 10^6 m^2/s). The heavy dashed lines are the 10 m/s contours of the zonal-mean zonal wind.

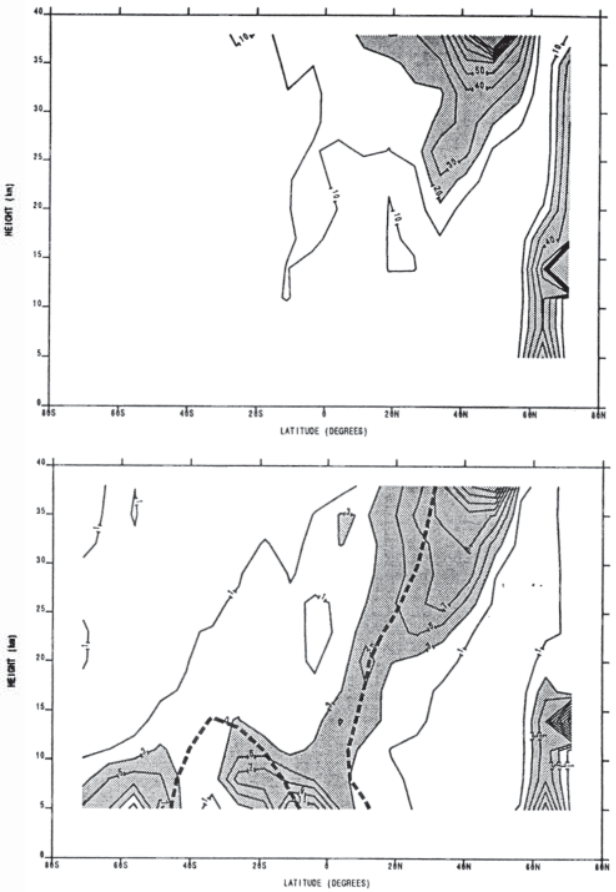

Figure 5. Latitude-height distribution of eddy mixing coefficients for the dusty solstice case: (top) K_{zz} (in units of 10 m^2/s) and (bottom) K_{yy} (in units of 10^6 m^2/s). The heavy dashed lines are the zero contours of the zonal-mean zonal wind.

(K_{yy} and K_{zz}), as depicted in Figures 4 and 5 for the near-equinox and dusty solstice cases. In all three of the experiments some of the determined values were negative, as was the case in the study of *Plumb and Mahlman* [1987]. The number of such values was relatively small (less than 5% in the equinox case, and only 10–15% in the dusty solstice case), and the mixing coefficients were set to minimum positive values (10^4 m^2/s for K_{yy}, and 1 m^2/s for K_{zz}) at all such grid points. The determinations of the mixing coefficients were noiser and more frequently negative at the lowest pressure level, and at the highest latitudes in the transport model. The plots in Figures 4 and 5 do not show the lowest level values nor the values at the highest two latitude grid points in each hemisphere.

In the near-equinox case the strongest eddy mixing tends to occur in lower latitudes, and the mixing is relatively symmetric about the equator. The largest values of both coefficients tend to lie in regions of relatively low zonal wind speeds, in the tropics and subtropics (the zonal wind field is qualitatively similar to that shown

in Figure 11 of *Haberle et al.* [1993]). Another region of strong mixing is present in middle and high northern latitudes at low levels, which is also in the vicinity of a zero mean-zonal wind line. There are midlevel (~10–25 km) maxima in both mixing coefficients, but the vertical mixing exhibits a strong maximum at higher levels (above ~30 km).

The distribution of the eddy mixing in the dusty solstice case is much less hemispherically symmetric, and much of the strongest mixing is found outside of the tropics. There are very large upper level maxima in both mixing coefficients (with K_{zz} values of more than 1000 m^2/s, and K_{yy} values exceeding 10^7 m^2/s) in the winter extratropics, and also low-level maxima in the meridional mixing in the summer hemisphere. All these areas of strong mixing are located in the vicinity of regions of relatively weak zonal winds, with the strong upper level mixing lying on the equatorward flanks of the intense winter westerly jet [see *Haberle et al.*, 1993, Figure 5]. The strong mixing at high northern latitudes and lower levels is also in an area of very weak zonal flow. It can be noted that the eddy mixing in the nondusty winter simulation (not shown) resembles that in the dusty case, but is weaker in magnitude (especially so in the northern subtropics at upper levels).

The tendency for much of the most vigorous mixing in the GCM experiments to occur in regions of relatively low zonal wind speeds strongly suggests that "breaking" of planetary eddies with relatively small phase speeds is taking place. Such breaking is a key to mixing processes in the Earth's stratosphere [e.g., *Plumb and Mahlman*, 1987]. Previous analyses of the Mars GCM simulations have shown that vigorous transient baroclinic eddies and quasi-stationary eddies are present in the extratropical winter hemisphere, and these extend to the model top [*Barnes et al.*, 1993, 1996]. Both types of eddies tend to reach maximum amplitudes in the uppermost model layers, in the solstice cases. There are also strong stationary eddy circulations in the summer hemisphere at solstice, but these are confined largely to lower levels [*Barnes et al.*, 1996]. In the near-equinox experiment the strong vertical eddy mixing concentrated in the tropics at upper levels is likely due in large part to the thermal tides, as these exhibit maximum amplitudes in this region and are relatively symmetric about the equator. Thermal tides (and/or other high-frequency motions) could also be a significant contributor to the strong mixing at upper levels in the winter extratropics in the dusty solstice simulation as well as to that at low levels in the summer hemisphere, as the tidal wind amplitudes are large in both of these regions.

The values of the off-diagonal components (K_{yz} and K_{zy}) of the eddy mixing tensor determined from the transport experiments are of significant magnitude: typical values are in the range of 10^3–10^4 m^2/s, there being a general increase in the values from the equinox case to the dusty solstice case (as for the K_{yy} and K_{zz} values). As discussed by *Plumb and Mahlman* [1987], the off-diagonal transport coefficients generally contribute to both the diffusive mixing and an advective transport. The latter contribution, associated with the antisymmetric part of the transport tensor, can be combined with the Eulerian mean meridional circulation to form the so-called transport circulation. The contribution to the diffusive mixing is contained in the symmetric part of the transport tensor, and these values are comparable with the K_{yz} and K_{zy} values in the results here. A timescale associated with this mixing can be estimated using both a vertical length scale and a meridional length scale; for a pressure scale height and a planetary radius, the timescales are then in the range of ~50–500 days. The symmetric part of the transport tensor can be diagonalized, so that the mixing is strictly diagonal ("purely diffusive") in the rotated coordinates. The results of doing this for the experiments here indicate that in some regions the eddy mixing is approximately one-dimensional, taking place along sloping surfaces in

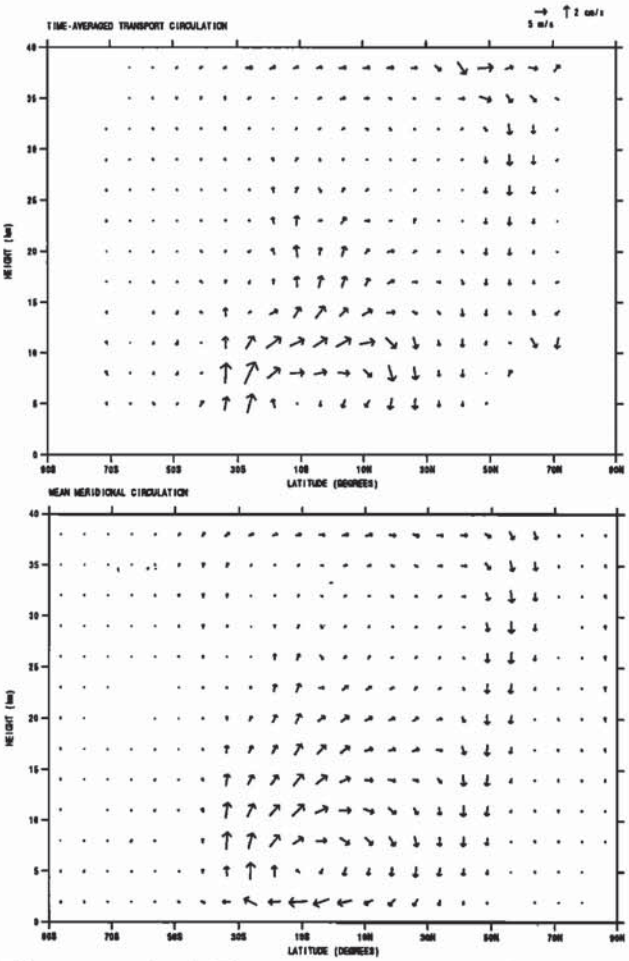

Figure 6. (top) The mean transport circulation and (bottom) the Eulerian mean circulation for the nondusty solstice experiment. The winds are depicted as arrows, whose directions are the appropriate ones for the horizontal and vertical scales of the plots.

the latitude-height plane. The major region where this is approximately the case is in middle and high winter latitudes, at lower and intermediate levels. This is a region where it is known that baroclinic eddies are very active in the GCM [*Barnes et al.,* 1993], and such eddies might be expected to produce such (strong) mixing. The slopes of the approximately one-dimensional mixing surfaces are of the order of the isentropic slopes in this region. However, in much of the GCM domain the mixing does not become nearly so one-dimensional in the principal coordinates of the diffusion tensor; the vertical mixing is still quite strong, of the same order as in latitude-height coordinates.

The advective eddy transport can be characterized in terms of a modification of the Eulerian mean advective transport, to yield the net transport circulation [see *Plumb and Mahlman,* 1987]. Figure 6 shows this circulation, as computed using the estimates of the off-diagonal transport coefficients (excluding the lowest pressure level and the two highest latitude grid points), for the nondusty solstice case, along with the Eulerian mean circulation for this case. It can be seen that the transport circulation is basically rather similar to the Eulerian mean circulation, though there are differences. In particular, there is stronger meridional flow at high levels in middle and high northern latitudes in the transport circulation, and the structure of the Hadley cell at midlevels and low latitudes is somewhat different. In both the equinox and dusty solstice cases, the transport circulation (not shown) is generally similar to the Eulerian mean circulation. The similarity is stronger for the very intense circulations in the dusty solstice case; in the equinox case, there are more sizeable differences (in particular, there is a stronger poleward meridional flow between ~5 and 10 km at middle and high latitudes in the northern hemisphere).

The computed transport circulations are also rather similar to the residual mean circulations, in all of the cases examined. In general, the residual mean circulations computed from GCM data bear a strong resemblance to the Eulerian mean circulations. *Haberle et al.* [1993] previously presented the residual mean circulation for a very dusty northern winter solstice simulation and compared it with the Eulerian mean circulation. The similarity between the transport and residual (and Eulerian mean) circulations in the GCM simulations is not a consequence of intrinsically weak eddy transports. Nor does it appear to be due to the eddies being nearly adiabatic, such that mixing occurs largely along isentropic surfaces [*Plumb and Mahlman,* 1987]. Instead, it appears to be largely due to the considerable strength of the Eulerian mean circulation (or equivalently, to the fact that the mean thermal structure is relatively close to that produced by the effects of diabatic heating and the mean circulation alone). In the equinox case the Eulerian mean circulation is relatively weak, and the differences between the various mean circulations appear to be larger than in the other cases.

4. Discussion

Idealized tracer transport experiments have been performed using wind fields produced by simulations with the NASA Ames Mars GCM. The results show that the strength of tracer transport varies tremendously with season and dust loading, being greatly intensified under dusty northern winter solstice conditions. In particular, the advective transport by the mean circulation becomes extremely rapid under such conditions, acting to ventilate the "stratosphere" ($p < 1$ mbar) in only about 1 week. For near-equinox conditions and a clear atmosphere, vertical eddy mixing processes appear to be dominant, as the mean ventilation timescales become quite long (~180 days). For the intermediate case of nondusty solstice conditions, mean advection and eddy mixing are of comparable importance. In all cases, stratospheric ventilation by the mean circulation and/or eddy mixing takes place on timescales that are very short by comparison with the Earth's stratosphere, where these timescales are of the order of a year or longer [e.g., *Shia et al.,* 1989]. The vertical eddy mixing (~20–100 m^2/s) is much stronger in all cases than that present in the bulk of the Earth's stratosphere, where a mixing coefficient value of 1 m^2/s is essentially an upper limit [e.g., *Shia et al.,* 1989; *Plumb and Mahlman,* 1987]. On the other hand, values of the meridional eddy mixing coefficient are fairly comparable to those appropriate for the Earth, at least in regions of relatively strong mixing [*Plumb and Mahlman,* 1987]. The much larger vertical eddy mixing must be due in sizeable part to the much greater diabatic heating rates in the Martian atmosphere (fundamentally a consequence of its low density and composition), with typical heating values being roughly an order of magnitude larger than the heating rates in Earth's stratosphere. The large radiative heating allows relatively rapid cross-isentropic transports of tracers, and drives large-amplitude thermal tides in the Martian atmosphere. In the simulations here, the transports due to the tides are associated with nonbreaking waves (since convective mixing is not incorporated), but the wind amplitudes in these are large and capable of producing very substantial vertical parcel dispersions. It also appears, though, that the transient and quasi-stationary eddies are important players in the vertical mixing. In connection with these eddies, it would seem that the very strong radiative damping in the Martian atmosphere must help to promote enhanced transports. Finally, an additional factor favoring stronger vertical mixing in the Martian regime is the existence of weaker vertical stratification than in Earth's stratosphere, though at higher latitudes this is not necessarily the case.

The model results obtained here can be compared with observational analyses. In particular, *Santee and Crisp* [1995] recently estimated a ventilation timescale of ~38 days for the region above 1 mbar, by computing a mean diabatic circulation from Mariner 9 IRIS data

for a late northern winter period ($L_s \sim 345°$). Analysis of a Mars GCM simulation for almost this same seasonal date and a dust optical depth of 0.3 yields a mean (Eulerian) ventilation timescale of ~45 days, in very good agreement with the Santee and Crisp result. The similarity between the Eulerian mean and diabatic mean (and residual mean) circulations in the GCM experiment makes this comparison a meaningful one.

The vertical eddy mixing in the GCM simulations is distinctly weaker than that (~10^3–10^4 m^2/s) inferred in some observational studies [e.g., *Conrath,* 1975; *Toon et al.,* 1977; *Anderson and Leovy,* 1978], and weaker than that employed in a number of photochemical modeling studies [e.g., *Kong and McElroy,* 1977; *Yung et al.,* 1988]. However, more recent photochemical studies have utilized weaker eddy mixing below ~30-50 km [e.g., *Atreya and Gu,* 1994; *Nair et al.,* 1994], as is evidenced by dust and ice haze analyses [*Kahn,* 1990; *Chassefiere et al.,* 1992; *Korablev et al.,* 1993]. The recent modeling study of *Rosenqvist and Chassefiere* [1995] attempts to bound the mixing coefficient values, and comes up with a globally averaged (0–80 km) "best estimate" of ~1000 m^2/s, substantially larger than a rough average of the more recent observational estimates (~100 m^2/s). The mixing values obtained here do not reflect the influence of convective mixing, and this would be expected to be present in the altitude regions where thermal tides and gravity waves are breaking (and below ~5–10 km, in the daytime convective boundary layer). Except under very dusty conditions, this wave breaking is probably largely confined to altitudes above ~40–50 km [e.g., *Zurek,* 1976; *Barnes,* 1990; *Joshi et al.,* 1995]. There is some observational evidence for the presence of sharp increases in the strength of the vertical eddy mixing in the ~40 to 50-km region [*Blamont and Chassefiere,* 1993]. The GCM simulations here indicate that relatively moderate vertical eddy mixing ($K_z \sim$ 20–100 m^2/s) is present in the 10 to 45-km region, but the modeled variation of this mixing with season, dustiness, and region in the atmosphere is very considerable. Under dusty solstice conditions, advective transport by the mean circulation becomes dominant and acts on very short timescales.

The mixing coefficient values obtained from the various observational analyses reflect, in general, the effects of both eddy mixing/advection and mean advection. The values obtained here reflect only the effects of the (large-scale) eddy processes. In the near-equinox case, in which the vertical eddy mixing is characterized by significantly faster timescales than the mean advection, the eddy mixing coefficient values should essentially be directly comparable with observational estimates. In the nondusty solstice case, where the mean advection and eddy mixing timescales are similar, the eddy mixing coefficients should still be roughly comparable with observational estimates (the latter should be roughly a factor of 2 larger than the model-purely eddy values). However, in the dusty solstice case the mean advection is the dominant process responsible for transport, and any observational estimates for such conditions should largely reflect transport by the mean circulation, assuming that the real transport processes below ~30–50 km on Mars are indeed primarily associated with mean overturning and not with eddy mixing. Values of the vertical mixing coefficient of $\sim 1 \times 10^3$ m^2/s correspond to mixing timescales of ~1 day (for a vertical length scale of a scale height), which are at least roughly comparable with the mean ventilation timescale obtained here for the dusty experiment. To be sure, the latter timescale has a somewhat different physical meaning than the eddy mixing timescale. *Holton* [1986] has proposed a formulation that allows the effects of a mean overturning to be expressed in terms of an equivalent vertical eddy mixing, for the global mean distribution of a tracer. In the limiting case of a conservative tracer, the effective mixing coefficient can be expressed as,

$$K_z \approx \frac{\overline{w}^2 a^2}{30 K_y}$$

where a is the planetary radius and $\overline{w}$ is the mean diabatic vertical velocity. Using a value of ~10 cm/s for this velocity in the dusty solstice case (and $\sim 2.5 \times 10^6$ m^2/s for K_y), the resulting value for K_z is about 1.5×10^3 m^2/s. The values for vertical mixing obtained by *Conrath* [1975] and *Toon et al.* [1977], which are of this order and appropriate for relatively dusty conditions, could thus largely reflect the effects of mean overturning and imply similar vertical transport to that obtained in the model study here. For the nondusty solstice case, Holton's expression for an effective mixing coefficient yields a value of ~50 m^2/s, comparable with the purely eddy values. For the equinox case, the resulting effective mixing coefficent value is only ~10 m^2/s, significantly smaller than the purely eddy values found here.

The tremendous variations in the tracer transport in the Mars atmosphere with season and atmospheric dust loading point to a need for models that attempt to incorporate such variability. This would seem to be especially true in the case of (e.g., photochemical) tracers that interact with and are influenced by the abundance and distribution of dust and water, both of which are known to vary seasonally and interannually to a large degree. On the other hand, it would certainly be of interest to attempt to investigate the net or average transports/mixing using annual and multi-annual simulations with GCM's.

Acknowledgments. This work was supported by a grant from the Planetary Atmospheres Program of NASA and a Cooperative Agreement with NASA Ames Research Center. J. Schaefer provided very valuable assistance with the computing at Ames. The authors would like to thank B.M. Jakosky and an anonymous reviewer for their very helpful comments, which led to a considerable improvement in the original manuscript.

References

Anderson, E., and C. B. Leovy, Mariner 9 television limb observations of dust and ice hazes on Mars, *J. Atmos. Sci., 35,* 723–734, 1978.

Atreya, S. K., and Z. G. Gu, Stability of the Martian atmosphere: Is heterogeneous catalysis essential?, *J. Geophys. Res., 99,* 13,133–13,145, 1994.

Barnes, J. R., Possible effects of breaking gravity waves on the circulation of the middle atmosphere of Mars, *J. Geophys. Res., 95,* 1401–1421, 1990.

Barnes, J. R., J. B. Pollack, R. M. Haberle, C. B. Leovy, R. W. Zurek, H. Lee, and J. Schaeffer, Mars atmospheric dynamics as simulated by the NASA Ames general circulation model, 2, Transient baroclinic eddies, *J. Geophys. Res., 98,* 3125–3148, 1993.

Barnes, J. R., R. M. Haberle, J. B. Pollack, and J. Schaeffer, Mars atmospheric dynamics as simulated by the NASA Ames general circulation model, 3, Quasi-stationary eddies, *J. Geophys. Res., 101,* 12,753-12,776, 1996.

Blamont, J. E., and E. Chassefiere, First detection of ozone in the middle atmosphere of Mars from solar occultation measurements, *Icarus, 104,* 324–336, 1993.

Chassefiere, E., J. E. Blamont, V. A. Krasnopolsky, O. I. Korablev, S. K. Atreya, and R. A. West, Vertical structure and size distributions of Martian aerosols from solar occultation measurements, *Icarus, 97,* 46–69, 1992.

Conrath, B. J., Thermal structure of the Martian atmosphere during the dissipation of the dust storm of 1971, *Icarus, 24,* 36–46, 1975.

Haberle, R. M., J. B. Pollack, J. R. Barnes, R. W. Zurek, C. B. Leovy, J. Murphy, H. Lee, and J. Schaeffer, Mars atmospheric dynamics as simulated by the NASA Ames general circulation model, 1, The zonal-mean circulation, *J. Geophys. Res., 98,* 3093–3123, 1993.

Holton, J. R., A dynamically based transport parameterization for one-dimensional photochemical models of the stratosphere, *J. Geophys. Res., 91,* 2681–2686, 1986.

Jakosky, B. M., and R. M. Haberle, The seasonal behavior of water on Mars, in *Mars,* edited by H. H. Kiefer et al., pp. 969–1016, Univ. of Ariz. Press, Tucson, 1992.

Joshi, M. M., B. N. Lawrence, and S. R. Lewis, Gravity wave drag in 3D atmospheric models of Mars, *J. Geophys. Res., 100,* 21,235–21,245, 1995.

Kahn, R., Ice haze, snow, and the Mars water cycle, *J. Geophys. Res., 95,* 14,677–14,693, 1990.

Kahn, R. A., T. Z. Martin, R. W. Zurek, and S. W. Lee, The Martian dust cycle, in *Mars,* edited by H. H. Kiefer et al., pp. 1017–1053, Univ. of Ariz. Press, Tucson, 1992.

Kong, Y., and M. B. McElroy, Photochemistry of the Martian atmosphere, *Icarus, 32,* 168–189, 1977.

Korablev, O. I., V. A. Krasnopolsky, A. V. Rodin, and E. Chassefiere, Vertical structure of Martian dust measured by solar occultations from the Phobos spacecraft, *Icarus, 102,* 76–87, 1993.

Matsuno, T., Lagrangian motion of air parcels in the stratosphere in the presence of planetary waves, *Pure Appl. Geophys., 118,* 189–216, 1980.

Murphy, J. R., J. B. Pollack, R. M. Haberle, C. B. Leovy, O. B. Toon, and J. Schaeffer, Three dimensional numerical simulations of Martian global dust storms, *J. Geophys. Res., 100,* 26,357–26,376, 1995.

Nair, H., M. Allen, A. D. Anbar, and Y. L. Yung, A photochemical model of the Martian atmosphere, *Icarus, 111,* 124–150, 1994.

Plumb, R. A., Eddy fluxes of conserved quantities by small-amplitude waves, *J. Atmos. Sci., 36,* 1699–1704, 1979.

Plumb, R. A., and J. D. Mahlman, The zonally averaged transport characteristics of the GFDL General Circulation/Transport Model, *J. Atmos. Sci., 44,* 298–327, 1987.

Pollack, J. B., R. M. Haberle, J. Schaeffer, and H. Lee, Simulations of the general circulation of the Martian atmosphere, 1, Polar processes, *J. Geophys. Res., 95,* 1447–1474, 1990.

Rosenqvist, J., and E. Chassefiere, A reexamination of the relationship between eddy mixing and O_2 in the Martian middle atmosphere, *J. Geophys. Res., 100,* 5541–5551, 1995.

Santee, M., and D. Crisp, The thermal structure and dust loading of the Martian atmosphere during late southern summer: Mariner 9 revisited, *J. Geophys. Res., 98,* 3261–3279, 1993.

Santee, M., and D. Crisp, Diagnostic calculations of the circulation in the Martian atmosphere, *J. Geophys. Res., 100,* 5465–5484, 1995.

Shia, R., Y. L. Yung, M. Allen, R. W. Zurek, and D. Crisp, Sensitivity study of advection and diffusion coefficients in a two-dimensional stratospheric model using excess carbon 14 data, *J. Geophys. Res., 94,* 18,467–18,484, 1989.

Toon, O. B., J. B. Pollack, and C. Sagan, Physical properties of the particles composing the Martian dust storm of 1971–1972, *Icarus, 30,* 663–696, 1977.

Toon, O. B., R. P. Turco, D. Westphal, R. Malone, and M. S. Liu, A multidimensional model for aerosols: Description of computational analogs, *J. Atmos. Sci., 45,* 2123–2143, 1988.

Yung, Y. L., J.-S. Wen, J. P. Pinto, M. Allen, K. K. Pierce, and S. Paulson, HDO in the Martian atmosphere: Implications for the abundance of crustal water, *Icarus, 76,* 146–159, 1988.

Zurek, R. W., Diurnal tide in the Martian atmosphere, *J. Atmos. Sci., 33,* 321–337, 1976.

J.R. Barnes and T.D. Walsh, College of Oceanic and Atmospheric Sciences, Oregon State University, 104 Ocean Admin Building, Corvallis, OR 97331-5503.

J.R. Murphy, NASA Ames Research Center, MS 245-3, Moffett Field, CA 94035-1000.

(Received August 31, 1995; revised January 10, 1996; accepted February 5, 1996.)